Electric-field-induced front deformation of Belousov-Zhabotinsky waves

Hana Ševčíková[1] and Stefan C. Müller[2]
[1]*Center for Nonlinear Dynamics of Chemical and Biological Systems, Prague Institute of Chemical Technology, Technicka 5, 166 28 Prague 6, Czech Republic*
[2]*Institut für Experimentelle Physik, Abteilung Biophysik, Otto-von-Guericke University, D-39016 Magdeburg, Germany*
(Received 24 April 1998; revised manuscript received 5 October 1998)

Experimental evidence is given of deformations in the vertical profiles of ferroin-catalyzed Belousov-Zhabotinsky waves propagating in thin horizontal cuvettes under an imposed dc electric field. While no deformations are seen in a zero field, for low negative field, or for any positive field, a pronounced S-shaped deformation does occur when a wave is exposed to a negative field above some critical magnitude. The observed phenomena are discussed on the basis of the convective flows that are assumed to increase in the negative field resulting from changes in the longitudinal profile of the wave. [S1063-651X(99)05507-5]

PACS number(s): 47.20.Bp, 47.70.Fw, 82.20.Mj, 66.30.Qa

I. INTRODUCTION

Belousov-Zhabotinsky (BZ) waves are a well-known example of reaction-diffusion pulse waves which can propagate in spatially distributed chemical systems with autocatalytic reactions [1,2]. It is also well known that imposing electric fields on such systems, causing the electromigration of the ionic reacting species, can substantially affect both the wave form and the velocity of propagation [3–10]. BZ waves are found to propagate faster against a gradient of electric potential and slower along it [4]. When moving in a gradient of electric potential of supercritical magnitude, BZ waves are subject to global electric-field-induced phenomena that account for (i) the splitting of new waves from the back of the existing one, (ii) the reversal of the direction of wave propagation, (iii) wave annihilation [4,8–10], and (iv) drift of spiral cores [6,7].

When traveling waves and the effects of imposed electric fields are studied, the reaction mixture is usually bound in a gel in order to prevent hydrodynamic flows in the system [6–10]. Convective flows have been measured in thin horizontal layers of the liquid phase BZ medium without an imposed electric field. Regular and irregular flow patterns have been shown to arise in very thin layers (0.85 mm deep) with an open liquid/gas interface [11] as a result of changes in surface tension induced by traveling wave trains [12]. In closed layers, which are considered here, the convective flows have been found to be very small in thin layers (mean velocity 1 $\mu m\,s^{-1}$ in a layer 1.5 mm deep) and to increase remarkably quickly with the layer thickness (mean velocity 20 $\mu m\,s^{-1}$ in a 3.5 mm layer) [13]. These flows were assumed to be responsible for the decomposition of target wave patterns into ''mosaic'' ones in the 3.5 mm layers. Indications of the onset of convection are also given by experimental observations of vertically propagating Mn^{2+}-catalyzed BZ waves in a tube of a somewhat larger inner diameter (4.3 mm) showing plumes arising at ascending waves while no deformations of wave profiles were observed in descending waves [14].

The destabilization of reaction-diffusion waves in liquid media has been widely reported for many other autocatalytic reacting systems such as iron (II)–nitric acid [15–17], arsenous acid–iodate [18–20], iodate-sulfite [21], and other reactions [22–24] supporting the propagation of front waves. Theoretical discussion [17,18,25] has shown that a density gradient can be established between the unreacted medium in front of the wave and the reacted medium behind the wave as a result of the production of heat and changes in the mixture composition during the course of the reaction. The density gradient thus created then induces a local convective flow that can cause a variety of distortions of the wave profiles depending on the system geometry and the nature of the density gradient in the particular reacting system [13–24].

In this paper, we report experimental observations of deformations of transverse profiles of ferroin-catalyzed BZ waves propagating in horizontal capillaries with the liquid medium under the influence of dc electric fields. We show that the virtually planar waves which propagate under zero field conditions become substantially deformed when the wave propagates towards the negative electrode. Conversely, no such deformations are observed when the wave propagates towards the positive electrode. The impact of wave profile deformation on the course of global electric-field-induced phenomena such as wave splitting and reversal [8,9] is demonstrated, and the conditions under which these global electric-field-induced phenomena maintain quasi-one-dimensionality are discussed. An attempt is made to explain the occurrence of wave deformations in an electric field on the basis of the increased local convective flows.

II. EXPERIMENTS

The experiments were carried out in the capillary reactor shown in Fig. 1(a). A quartz-glass rectangular cuvette (GC) with outer dimensions $9\times9\times84\,mm^3$ forms the main part of the reactor. The cuvette, fitted into two filling chambers (FC), is mounted between two electrolytic cells (EC) equipped with platinum plate electrodes (PE). The cuvette and both electrolytic cells are filled with the same reaction solution that consists of 0.205*M* $HBrO_3$, 0.007*M* NaBr, 0.05*M* malonic acid, and 0.002*M* ferroin (the same as in previously reported experiments on electric-field effects [8,9].) Custom-made Teflon membranes (TM), placed between each of the filling chambers and electrolytic cells, al-

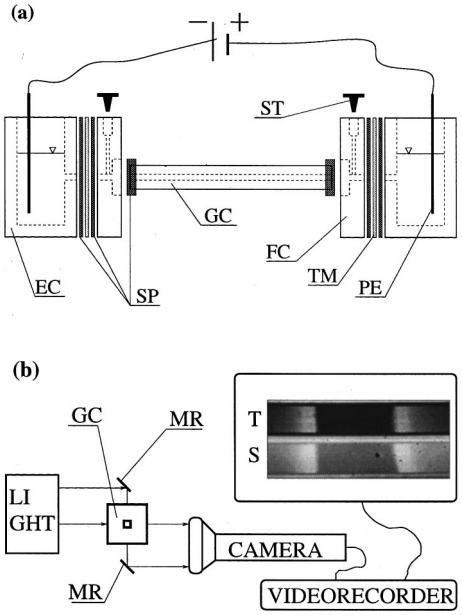

FIG. 1. (a) Scheme of the experimental setup. GC—rectangular glass cuvette (inner cross section: 0.5×0.5, 0.7×0.7, or $1\times1\ \mathrm{mm}^2$, outer cross section: $9\times9\ \mathrm{mm}^2$; length: 84 mm); EC—electrolytic cells; FC—filling chambers; SP—silicon packings; TM—microporous Teflon membranes; PE—platinum electrodes; ST—stoppers. (b) Monitoring arrangement. GC—glass cuvette; MR—mirrors; *S*—side and *T*—top view of the cuvette with the vertical and the horizontal profiles of the traveling waves, respectively. (Two waves approaching each other in the 1 mm cuvette are shown. The lightest zones mark the excited regions, the dark region between them corresponds to unreacted medium, gray zones on the left and right of the snapshot represent refractory regions.)

low for migration of ions when an electric field is switched on and, at the same time, eliminate possible macrohydrodynamical flows through the cuvette. After the cuvette is filled with the reaction solution, the openings of both filling chambers are tightly closed by stoppers (ST) in order to eliminate CO_2 bubble formation by the BZ reaction in the cuvette. The whole reactor is then placed in a water bath thermostated at 15 °C.

Oxidation waves were spontaneously generated at both ends of the cuvette and propagated into it. Each experiment lasted about 2 hours on average. During that time either one, two, or three subsequent waves were formed at the ends. Wave generation is rather random and the number of waves generated is also affected by the applied electric field, which facilitates wave initiation at the end closer to the negative electrode and suppresses it at the opposite end. The waves propagate with constant velocities both under the effects of an electric field and without it (cf. also [4]) and their velocities are in the order of millimeters per minute (cf. also [4]).

The waves were followed visually utilizing the difference in light absorption between the reduced and oxidized parts of the reacting medium. A light beam was split by mirrors into two beams passing through the cuvette in vertical and horizontal directions (transverse to the longitudinal axis), see Fig. 1(b). Both horizontal and vertical profiles of the pulse wave were thus monitored simultaneously (by a Hamamatsu C1000 video camera) and recorded on videotape. The optical setup allows the monitoring of approximately 8.5 mm of the cuvette length (with a spatial resolution of about 17 μm per pixel). The recorded images were digitized and processed by various commercial software programs to obtain data for further evaluation. Several FORTRAN77 codes have been developed to evaluate the velocities of the propagating waves and to measure the changes in wave deformation and width.

III. RESULTS

The following convention is used throughout: the electric field (the applied voltage) is referred to as positive when a wave propagates towards the positive electrode (i.e., against the gradient of electric potential) and as negative when a wave propagates towards the negative electrode (i.e., in the direction of the electric potential gradient). As the intensity of electric field (E) is directly related to the applied voltage U ($E=U/d$, where d is the fixed distance between the electrodes) the value of the applied voltage is used to represent the electric-field strength.

Three rectangular cuvettes of different inner cross sections (namely, $0.5\times0.5\ \mathrm{mm}^2$, $0.7\times0.7\ \mathrm{mm}^2$, and $1\times1\ \mathrm{mm}^2$) were used to investigate the stability of the transverse profile of BZ waves propagating in the applied electric field. The transverse profiles of the wave front are essentially planar in all three cuvettes when no electric field is applied. However, slight random deviations from planar of the vertical profile are observed.

Typical wave profiles without an imposed field are illustrated in Fig. 1(b) in a snapshot of two counterpropagating waves in the 1 mm cuvette. The horizontal profiles of both waves are planar but differences in their vertical profiles are visible. The vertical profile of the left wave appears planar while the one on the right is slightly tilted with its top ahead of the bottom. Other forms of vertical profile deformation were also observed, including slightly convex or concave shapes or tilted fronts with either the bottom or top preceding. The deformations are evaluated as the distance between the most advanced and the most retarded part of the wave front and expressed as a percentage of the inner width of the cuvette. They vary from 5% to 11% for the 0.5 mm cuvette and from 5% to 17% for the 1 mm cuvette. The deformation of the horizontal profiles was found to be at most 5% and it is this value that we ascribe to the noise in the recorded data. In spite of these slight random deformations the reaction front always occupies the whole cuvette cross section. Thus the wave propagation can be regarded essentially as a one-dimensional process.

The effects of applied dc electric fields of constant magnitude on the shape of the horizontal and the vertical profiles of BZ waves are illustrated in Fig. 2. In Fig. 2(a) a wave propagates from right to left in a zero field exhibiting a planar profile in the horizontal direction and a slightly tilted profile in the vertical direction with the upper part preceding the lower one. When a positive voltage ($U=+50\ \mathrm{V}$) is applied, the wave accelerates ($v_0=1.46\ \mathrm{mm/min}$ and $v_{+50\ \mathrm{V}}=1.766\ \mathrm{mm/min}$) with the transverse profile remaining planar [Fig. 2(b)]. When a negative voltage is applied ($U=-90\ \mathrm{V}$), the wave slows down ($v_0=1.03\ \mathrm{mm/min}$ and $v_{-50\ \mathrm{V}}=0.65\ \mathrm{mm/min}$) and the vertical profile adopts an S shape with the bottom part preceding the top part [Fig. 2(c)]. After the voltage is switched off, the vertical wave profile

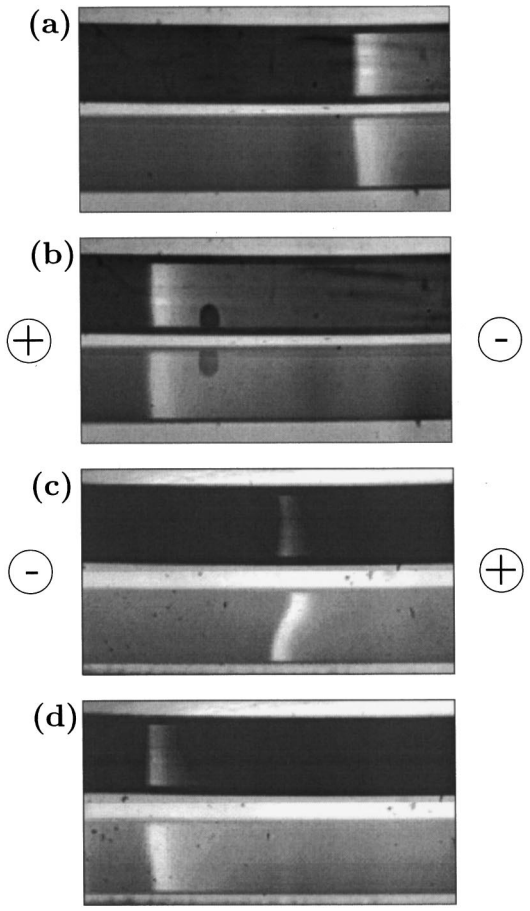

FIG. 2. Horizontal (upper row) and vertical (lower row) BZ wave profiles for different applied voltages: (a) $U=0$ V, (b) 2 min after switching on the positive voltage ($U=50$ V), (c) 2 min after switching on the negative voltage ($U=-50$ V), and (d) 45 s after switching off the voltage again. Cases (a), (b) and (c), (d) show two different experimental runs performed in the 1 mm cuvette.

becomes planar again after a transition period of the order of 60 s, as shown in Fig. 2(d). No changes in the shape of the horizontal profile were observed in either positive or negative fields.

Wave deformation by negative fields of increasing strength occurs in a stepwise manner, i.e., there is no visible difference between the shape of the wave profile in a zero and a negative field of a subcritical strength. However, when a field of a supercritical strength is applied, the vertical profile of the wave adopts a pronounced S shape with the bottom preceding the top. The value of this critical field strength depends on the size of the cuvette inner cross section; critical voltages about -50 and -80 V were found for the 1 mm and 0.5 mm cuvettes, respectively. This is illustrated in Fig. 3 where the dependence of wave profile deformation on the magnitude of the applied voltage is drawn schematically.

It is not only the vertical transverse profiles of BZ waves that are subject to changes when the wave is exposed to an external electric field but their longitudinal profiles as well. In Fig. 4 the longitudinal profiles of waves traveling in zero and -90 V fields are compared (the profiles are taken from the side view snapshots at the center of the cuvette). The rise and fall of the transmitted light intensity corresponds to the front and back of the BZ pulse wave, respectively. Both the

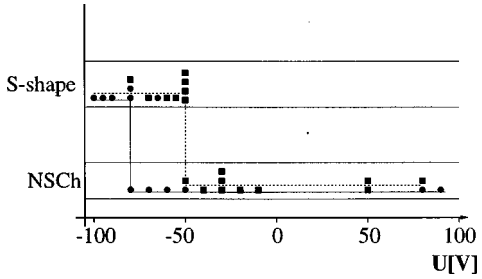

FIG. 3. The occurrence of a deformation of the vertical profile, depending on the electric voltage in the 0.5 mm (●) and 1 mm (■) cuvettes. The S-shaped row collects the experiments in which the wave adopts an S shape after the voltage is switched on, the NSCh row shows the observations with no significant change of the wave profile after switching on the voltage.

wave front and wave back are clearly sharper in the negative than in the zero electric field. Also, the width of the excited zone (measured as the distance between the wave front and back at some constant light intensity I_{ref}) is smaller in the negative field than when no electric field is applied. For the case shown in Fig. 4 the wave width in a zero field is 0.74 mm, that in a -90 V electric field is 0.53 mm; i.e., the wave width decreases by about 30%. The changes in the form of the longitudinal profile observed in this liquid reaction system are qualitatively the same as those observed in a gelled reaction mixture of the same composition [8].

The adjustment of the vertical profile of the wave, after the negative electric field is switched on, is documented in Fig. 5 in a series of black and white images taken from the video-recorded experiment [Fig. 5(a)]. A related contour plot [Fig. 5(b)] enables us to trace changes in the wave width,

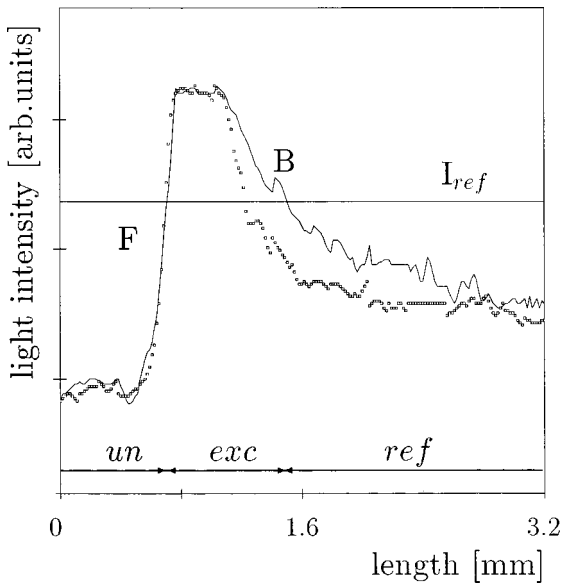

FIG. 4. Longitudinal profiles of BZ wave in zero (full line) and in negative (dotted line) electric fields in the 0.7 mm cuvette, applied voltage $U=-90$ V. The light intensity (in arbitrary units) is a measure of the concentration of ferriin. The letters $F(B)$ denote the wave front (back); un, exc, and ref denote unreacted, excited, and refractory regions, respectively. The profiles were taken from the same experiment as that of Fig. 5 at times 20 and 65 s and superimposed.

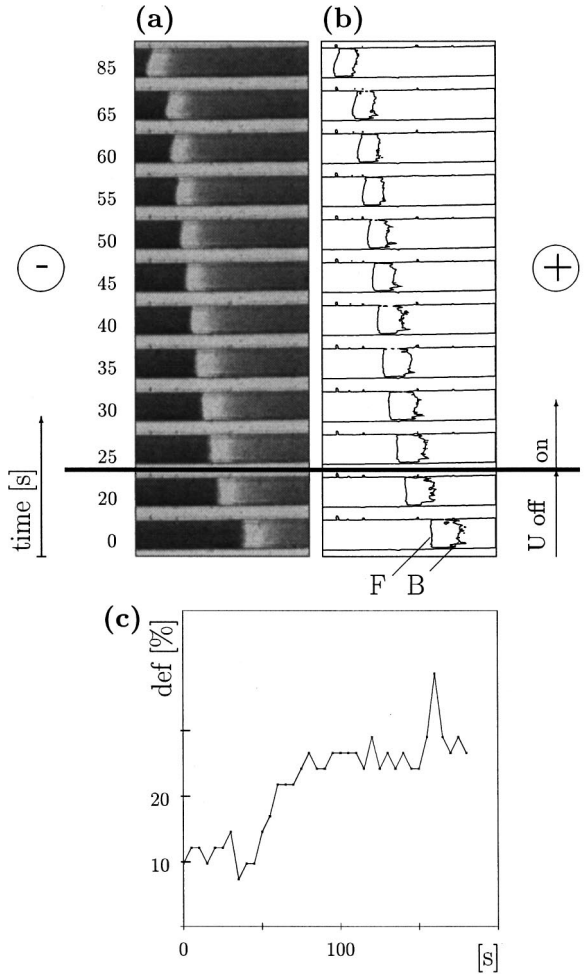

FIG. 5. Development of the vertical profile deformation and the wave width under a negative electric field (0.7 mm cuvette, applied voltage $U=-90\,\mathrm{V}$). (a) Series of images, (b) a contour plot tracing the constant level of light intensity I_{ref}. Numbers on the left show the time elapsed after the first image. (c) Increase in the wave front deformation (expressed as a percentage of the cuvette width) in the imposed electric field as a function of time.

visualized as the distance between contours tracing the reference light intensity at both the wave front and the wave back (labeled as *F* and *B*). The first two images (time 0 and 20 s) show the shape of the pulse wave in a zero electric field. The electric field is switched on at the time 21 s. It takes about 30 s until a decrease in the width of the wave is visible and the vertical deformation starts to develop (time 50 s). The dependence of the wave front deformation on time [Fig. 5(c)] shows that, in this particular case, the transition time for the deformation to reach a constant value is about 60 s. We can also see that the wave width gets smaller as the wave front deformation evolves in time.

The transverse deformations of the wave profiles have a remarkable impact on the course of global electric-field-induced phenomena that account for wave splitting, reversal, and annihilation [8,9]. In a BZ medium that is embedded in agar gel [8] these global changes occur in a quasi-one-dimensional manner, i.e., simultaneously at all locations across the cross section of the cuvette. In a liquid medium the situation is different and depends on how quickly the global change in the wave behavior occurs in comparison

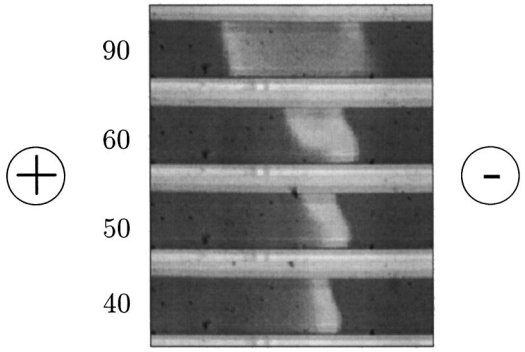

FIG. 6. Wave reversal in a negative electric field (0.7 mm cuvette, applied voltage $U=-100\,\mathrm{V}$). Numbers give the time (in seconds) elapsed after switching the voltage on. Vertical profiles are shown.

with the transition time needed for the S-shaped deformation to develop. On average, wave deformation becomes evident approximately 30 s after the voltage is switched on. Therefore, if the global change is accomplished quickly (within 30 s), no deformation develops and the global phenomenon occurs in a quasi-one-dimensional fashion (as if it were performed in agar gel). This type of behavior was often observed in connection with wave annihilation in all three cuvettes and in some cases of wave reversal in the 0.5 mm capillary. However, in the majority of cases of wave reversal and splitting, the global change occurs slowly (between 30 and 180 s) leaving sufficient time for the S-shaped deformation to develop. The temporal evolution of the global change then varies along the vertical dimension of the cuvette as illustrated in Figs. 6 and 7.

The global change shown in Fig. 6 corresponds to a wave reversal because, in the course of time, the original wave ceases to exist and a new wave formed at its back propagates in the opposite direction. The first image shows the vertical shape of the wave moving to the right 40 s after the negative voltage ($U=-100\,\mathrm{V}$) was applied. The wave front is distinctively S shaped and the wave back appears tilted rather than S shaped. During the next 10 s the excited zone becomes wider at the upper part of the cuvette as the wave back starts to propagate backwards. A new wave front then emerges from the wave back and grows towards the bottom of the cuvette (next image). Finally, the wave occupies the whole cross section and propagates to the left (the final image). In the course of wave reversal the S-shaped deformation of the original wave increases and eventually this wave vanishes; this process proceeds from the bottom of the cuvette to the top.

Figure 7(a) demonstrates the course of wave splitting in the 1 mm cuvette. The first image [Fig. 7(a), time 90 s] shows the vertical profile of a wave moving to the left that has developed an S-shaped form after the negative voltage ($U=-50\,\mathrm{V}$) was switched on. The deformation of the profile increases with time and a new wave emerges from the back of the original wave at the top of the cuvette (time 130 s). The new wave propagates to the right and to the bottom (times from 150 to 210 s) and soon extends over the whole cross section of the cuvette (time 230 s) and becomes planar (time 270 s) as the wave propagates in the positive field. The original wave slowly ceases to exist, starting from the bot-

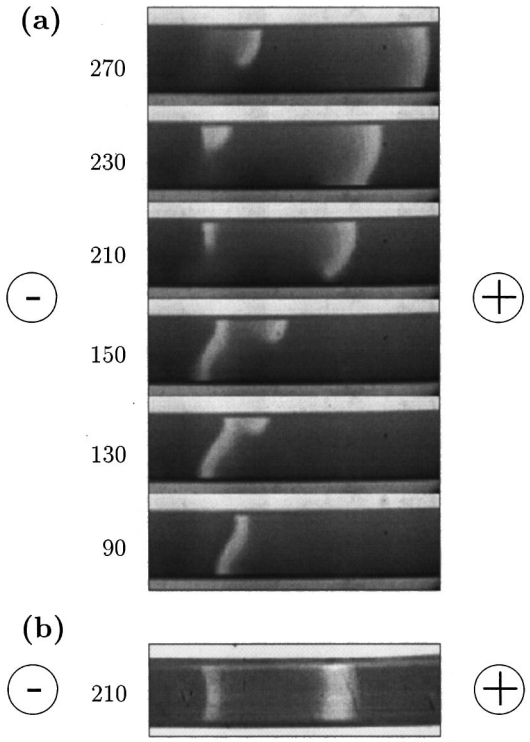

FIG. 7. Wave splitting in a negative electric field (1 mm cuvette, applied voltage $U=-50$ V). Numbers give the time (in seconds) elapsed after switching the voltage on. (a) Series of vertical profiles; (b) the horizontal profile corresponding to the vertical profile at 210 s.

tom and progressing to the top (times from 150 to 270 s). A second new wave emerges from the remainder of the excited zone of the original wave at the top of the cuvette (time 230 s) and propagates to the right and to the bottom (time 270 s). The free ends of both new waves show a tendency to curl up but the formation of a spiral is suppressed by the negative electric field acting on these free ends [9,10]. The corresponding view of the horizontal profile of the waves [Fig. 7(b)] illustrates that no significant variations in the course of the wave splitting occur along the horizontal direction of the cuvette. This suggests that new waves emerge from the back of the original wave as scroll waves [26] with the filaments orientated along the horizontal direction. Each filament is formed at the top of the cuvette and, as the wave propagates, it moves to the right and to the bottom. Finally, it touches the bottom and ceases to exist. Thus only one involute of the elongated spiral [26] is formed, giving rise eventually to only one planar wave.

IV. DISCUSSION

The observations reported above document the pronounced deformations of the vertical transverse profile of BZ waves when they are exposed to supercritical magnitudes of negative electric fields. The wave deformations were observed in all the three cuvettes used (inner cross sections: 0.5×0.5, 0.7×0.7, or 1×1 mm^2) and the extent of the deformation was found to reach up to 60% of the cuvette width for the cuvette with the largest cross section.

As the deformations occur only in the vertical direction, the assumption can be made that this wave deformation is gravity dependent. Assuming that horizontal density gradients exist across the BZ wave [14,25] we can account for wave profile deformation in terms of a convective instability. In ferroin-catalyzed BZ systems, the density of excited region is higher than the density of the unreacted region and thus the fluid will flow in the opposite direction to the propagating wave in the upper part of the cuvette and in the same direction as it in the lower part [25]. This results in a slanted (S-shaped) vertical wave profile with the bottom part preceding the top, which is the shape of the wave profile observed in supercritical negative fields. The question then arises as to why the waves are deformed only in such fields and not in zero, low negative, or any positive electric fields.

As the wave profiles in a zero applied field are essentially planar we may conclude that the driving force for convection (the density gradient) is small and insufficient to cause any observable wave deformation. This agrees well with the results of experiments [13] in which very small convective flows ($1\ \mu$m s^{-1}) were measured in horizontal layers of BZ medium of thickness 1.5 mm, where they caused only minor distortions of traveling BZ wave patterns. Since no disturbances of target patterns were observed in the layers thinner than 1 mm [13], we can assume that the convective flows are insignificant in these layers.

Simulation studies of convective effects on wave propagation in the BZ system with Oregonator kinetics [27] have shown that the velocity of wave propagation in horizontal slabs does not significantly increase with the slab thickness until the thickness reaches a certain critical size, thereafter it increases rapidly with slab thickness. The critical size found was 0.2 mm and for this slab the velocity of the wave propagation increased by 0.4% with respect to the pure reaction-diffusion velocity[27]. This means that the velocity of the convective flow, which adds to the pure reaction-diffusion velocity [18], is negligible and we can assume that such a flow will not affect the shape of the wave. Thus, although convection is expected to be always present in media with horizontal density gradients [28] we can conclude that, from the experimental point of view, the effects of induced convection on wave propagation are not detectable until the horizontal slab is thicker than a certain critical size. Our observations indicate that, in the case of BZ waves, the 1 mm cuvette is still below this critical value when no electric field is applied since the transverse vertical wave profiles are virtually planar.

We now speculate on the possible reason why the transverse vertical profiles deform when BZ waves are subject to external negative electric fields of supercritical magnitudes. Following on from what has been said above, we assume that it is the velocity of the convective flow that increases in the negative field and causes the wave profile deformation. The expression for the average flow velocity in a horizontal cylinder with a propagating chemical front wave has been derived in [18] as

$$\langle v\rangle=\frac{1}{32}\frac{r_0^4 g}{\mu}\left[\frac{\Delta\rho_c}{L_c^2}+\frac{\Delta\rho_T}{L_T^2}\right], \tag{1}$$

with $\langle v\rangle$ being the average flow velocity, r_0 the cylinder radius, g the acceleration in the gravitational field, μ the

viscosity, $\Delta\rho_c$ ($\Delta\rho_T$, respectively) the density difference between the unreacted and reacted medium caused by compositional (temperature, respectively) changes during the reaction, and $L_{c,T}$ the distance over which the respective density difference occurs. Relation (1) builds on the expression for the velocity of a convective flow in the midplane of the horizontal cylinder where the horizontal density gradient is established by holding the ends of the cylinder at different temperatures [29].

As opposed to front waves, where only one spatial density gradient between two different regions (reacted and unreacted) has to be considered, two spatial density gradients must be taken into account in the case of BZ pulse waves; one arising across the wave front and the other across the wave back. According to the assumed changes in the density during the reaction [25], these two gradients have opposite signs and, in general, will set up two counter-rotating convective rolls [27]. However, due to the chemical coupling between the wave front and the wave back, the effect of these two rolls on the shape of the wave profile becomes a rather complex function of the system geometry and the magnitude of the density changes [27].

Applying relation (1) to our case, with r_0 now representing the half-width of the cuvette, we can see that the velocity of the convective flow increases with the width of the tube, with the increased density difference, and with the decreased length over which the density difference exists. A dc electric field does not affect either the physical properties of the medium or the reaction kinetics, i.e., we assume μ and $\Delta\rho_{c,T}$ remain constant. What does change in an electric field is the shape of the longitudinal wave profile (Ref. [8] and Fig. 4). The sharpening of both the wave front and the wave back in negative fields leads to decreasing values of $L_{c,T}$ across both the wave front and the wave back and, consequently, to the increase of the velocity of convective flows. Even if only one overall density gradient is assumed to be responsible for the wave deformation as in [14] the distance over which it occurs, the width of the wave, becomes smaller in the negative electric fields (Fig. 4), resulting in the increase of the convective flow. In this way convection may become more pronounced in negative fields and may cause the wave profile deformation.

In positive fields, the longitudinal profile of the wave is more spread out than in negative and zero electric fields situations [8]. Thus $L_{c,T}$ increases and the velocity of the convective flow will be even smaller than in the case without an imposed electric field. As a result, the wave profile does not visibly deform in positive fields.

We can also intuitively presume that the effect of convection on the shape of the transverse wave profile will increase not only with the absolute value of the velocity of the convective flow but also with the increased ratio of the convective and wave propagation velocities. This ratio increases in negative electric fields, which slow down the wave propagation, and thus convection becomes sufficiently strong to cause the deformation of the transverse vertical profile of the wave.

Experimental results (Fig. 3) suggest that a higher negative field is needed to deform the wave profile in smaller cuvettes. This is in agreement with relation (1) that predicts the increased velocity of convective flow for increased cuvette width. This leads to the assumption that there will be a correlation between the strength of the negative field and the critical size of the cuvette below which convection will have no detectable effect on the wave profile. However, this assumption calls for confirmation by additional measurements.

ACKNOWLEDGMENTS

It is a great pleasure to thank Martin Böckmann for many inspiring discussions, Jana Karbanová for help in processing the video-recorded data, and John Merkin for English corrections. Partial financial support by the Czech Ministry of Education (Grant No. VS 96703) is also acknowledged.

[1] *Oscillations and Travelling Waves in Chemical Systems*, edited by R. J. Field and M. Burger (Wiley-Interscience, New York, 1985).
[2] *Chemical Waves and Patterns*, edited by R. Kapral and K. Showalter (Kluwer Academic, Dordrecht, 1995).
[3] R. Feeney, S. L. Schmidt, and P. Ortoleva, Physica D **2**, 536 (1981).
[4] H. Ševčíková and M. Marek, Physica D **9**, 140 (1983).
[5] H. Ševčíková and M. Marek, Physica D **13**, 379 (1984).
[6] O. Steinbock, J. Schütze, and S. C. Müller, Phys. Rev. Lett. **68**, 248 (1992).
[7] K. I. Agladze and P. DeKepper, J. Phys. Chem. **96**, 5239 (1992).
[8] H. Ševčíková, M. Marek, and S. C. Müller, Science **257**, 951 (1992).
[9] H. Ševčíková, I. Schreiber, and M. Marek, J. Phys. Chem. **100**, 19 153 (1996).
[10] H. Ševčíková, J. Kosek, and M. Marek, J. Phys. Chem. **100**, 1666 (1996).
[11] H. Miike, S. C. Müller, and B. Hess, Phys. Lett. A **144**, 515 (1988).
[12] K. Matthiessen, H. Wilke, and S. C. Müller, Phys. Rev. E **53**, 6056 (1996).
[13] J. Rodriguez and C. Vidal, J. Phys. Chem. **93**, 2737 (1989).
[14] M. Menzinger, A. Tzalmona, R. L. Armstrong, A. Cross, and D. Lemaire, J. Phys. Chem. **96**, 4725 (1992).
[15] G. Bazsa and I. R. Epstein, J. Phys. Chem. **89**, 3050 (1985).
[16] I. Nagypál, G. Bazsa, and I. R. Epstein, J. Am. Chem. Soc. **108**, 3635 (1986).
[17] J. A. Pojman, I. P. Nagy, and I. R. Epstein, J. Phys. Chem. **95**, 1306 (1991).
[18] J. A. Pojman, I. R. Epstein, T. J. McManus, and K. Showalter, J. Phys. Chem. **95**, 1299 (1991).
[19] J. Masere, D. A. Vasquez, B. F. Edwards, J. W. Wilder, and K. Showalter, J. Phys. Chem. **98**, 6505 (1994).
[20] M. R. Carey, S. W. Morris, and P. Kolodner, Phys. Rev. E **53**, 6012 (1996).
[21] A. Keresztessy, I. P. Nagy, G. Bazsa, and J. A. Pojman, J. Phys. Chem. **99**, 5379 (1995).

[22] I. P. Nagy and J. A. Pojman, J. Phys. Chem. **97**, 3443 (1993).
[23] C. R. Chinake and R. H. Simoyi, J. Phys. Chem. **98**, 4012 (1994).
[24] I. P. Nagy, A. Keresztessy, J. A. Pojman, G. Bazsa, and Z. Noszticzius, J. Phys. Chem. **98**, 6030 (1994).
[25] J. A. Pojman and I. R. Epstein, J. Phys. Chem. **94**, 4966 (1990).
[26] A. T. Winfree, S. Caudle, G. Chen, P. McGuire, and Z. Szilagyi, Chaos **6**, 617 (1996).
[27] Y. Wu, D. A. Vasquez, B. F. Edwards, and J. W. Wilder, Phys. Rev. E **51**, 1119 (1995).
[28] E. L. Cussler, *Diffusion. Mass Transfer in Fluid Systems* (Cambridge University Press, Cambridge, England, 1984).
[29] P. Bontoux, B. Roux, G. H. Schiroky, B. L. Markham, and F. Rosenberger, Int. J. Heat Mass Transf. **29**, 227 (1986).